Biosensors and Bioelectronics ■ (■■■■) ■■■–■■■

Contents lists available at ScienceDirect

Biosensors and Bioelectronics

journal homepage: www.elsevier.com/locate/bios

Nanoplasmonic biosensor: Coupling electrochemistry to localized surface plasmon resonance spectroscopy on nanocup arrays

Diming Zhang [a], Yanli Lu [a], Jing Jiang [b], Qian Zhang [a], Yao Yao [a], Ping Wang [a], Bilian Chen [c], Qiaoyuan Cheng [c], Gang Logan Liu [b], Qingjun Liu [a,d,*]

[a] Biosensor National Special Laboratory, Key Laboratory for Biomedical Engineering of Education Ministry, Department of Biomedical Engineering, Zhejiang University, Hangzhou 310027, PR China
[b] Micro and Nanotechnology Lab, University of Illinois at Urbana-Champaign, IL 61801, USA
[c] Zhejiang Institute for Food and Drug Control, Hangzhou 310014, PR China
[d] Cyber Innovation Joint Research Center, Zhejiang University, Hangzhou 310027, PR China

ARTICLE INFO

Article history:
Received 24 May 2014
Received in revised form
11 August 2014
Accepted 14 August 2014

Keywords:
Localized surface plasmon resonance (LSPR)
Nanoscale cup arrays (nanoCA)
Electrochemistry
Cyclic voltammetry (CV)
Biosensor

ABSTRACT

The nanoscale Lycurgus cup arrays were hybrid structures of nanocups and nanoparticles with ultrasensitivity to refractive index change. In this study, an electrochemical localized surface plasmon resonance (LSPR) sensor was developed by coupling electrochemistry to LSPR spectroscopy measurement on the nanoscale cup arrays (nanoCA). Based on the combination of electrochemistry and LSPR measurement, the electrochemical LSPR on nanoCA was observed with significant resonance wavelength shifts in electrochemical modulation. The synchronous implementation of cyclic voltammetry and optical transmission spectrum can be used to obtain multiply sensing information and investigate the enhancement for LSPR from electrochemical scanning. The electrochemical enhanced LSPR was utilized as biosensor to detect biomolecules. The electrochemical LSPR biosensor with synchronous electrochemical and optical implement showed higher sensitivity than that of conventional optical LSPR measurement. Detecting with multi-transducer parameters and high sensitivity, the electrochemical LSPR provided a promising approach for chemical and biological detection.

1. Introduction

Surface plasmon resonance (SPR) is one of the most widespread sensor techniques to monitor various events taking place on a metal film. It has emerged as a powerful label-free method to study molecular binding processes on the sensor surface. These SPR sensors are mostly measured in optical refractometric method and respond to refractive index (RI) changes from analyte binding on the sensor. A lot of groups have reported applications of SPR sensors for analyte detections, ranging from chemical to biological molecules, by utilizing specific conjunctions on the surface of those sensors (for reviews see Homola (2008) and Tokel et al. (2014)). However, SPR is not only influenced by RI change on the surface, but also modulated by potential and current density on the surface of metal film (Sannomiya et al., 2010; Wang et al., 2010; Zhang et al., 2007). Thus, SPR sensors are combined with electrochemistry in implement of synchronized electrical and optical responses. These electrochemical SPR sensors often employ metal film as working electrode and detect changes in peak position or width of optical plasmonic spectroscopy for electrochemical processes (Baba et al., 2010; Shan et al., 2012; Yu et al., 2014). The combination of electrochemistry and optical SPR measurement can provide multiply information from different signal transductions and provide novel approaches to elucidate detailed processes for electrochemical reactions. The synergetic electrochemical and SPR effect can also be used to control surface functionalizations of sensor devices and molecular binding during bio-measurements (Cheng et al., 2014; Liron et al., 2002; Pallarola et al., 2013).

SPR stimulated on nanoscale structures is nonpropagating or propagating within limited volume on device surface and thus often named as localized surface plasmon resonance (LSPR) (Mayer and Hafner, 2011; Zeng et al., 2011). Nanostructure devices with LSPR have special electrical and optical properties that can be used in various novel applications. During the last decade, nanoplasmonic sensors based on various nanostructures (e.g. nanoparticles, nanorods, nanoshells and nanoholes) have attracted much attention in the field of chemical and biological sensing (Cao et al.,

* Corresponding author at: Biosensor National Special Laboratory, Key Laboratory for Biomedical Engineering of Education Ministry, Department of Biomedical Engineering, Zhejiang University, Hangzhou 310027, PR China.
Tel.: +86 571 87952832; fax: +86 571 87951676.
E-mail address: qjliu@zju.edu.cn (Q. Liu).

http://dx.doi.org/10.1016/j.bios.2014.08.022
0956-5663/

2014; Stewart et al., 2008). Similar to SPR detection, these LSPR sensors can also respond to RI changes on nanostructures in position or width of LSPR optical spectrum. However, different from SPR sensors, the nanostructured sensors based on LSPR usually employ straight light coupling directly and do not need complex optical path coupling like Kretschmann configuration. The simple and miniaturized light path designs in sensing apparatus make LSPR sensors be promising optical plasmonic platforms for biochemical detections. In our previous work, nanoscale Lycurgus Cup arrays were fabricated with hybrid structures of nanocups and nanoparticles (Gartia et al., 2013). It can overcome some drawbacks of conventional nanostructures, such as multiply LSPR peaks of nanoholes and difficult size control for nanoparticles. More importantly, it has unprecedented high sensitivity in detecting small changes in RI of analyte. Thus, considering the wide applications of electrochemical SPR, it is a meaningful work to fabricate electrochemical LSPR sensor on the nanocups with synchronous electrochemical and optical LSPR measurement for bio-detection.

Here, we first developed an electrochemical LSPR biosensing platform by coupling electrochemical scanning to LSPR on nanoscale cup arrays (nanoCA). The LSPR features and electrochemical properties of nanoCA were evaluated respectively. Then, electrochemical LSPR was measured in transmission spectrum and electrochemical scanning. The interactions of LSPR and electrochemical current were observed and analyzed in the synergetic measurement. Finally, the electrochemical LSPR was applied in detection for biomolecules with electrochemical enhancement for LSPR on the nanocups. The electrochemical LSPR biosensor was demonstrated to have greater response and higher sensitivity than those of conventional optical measurement.

2. Experiments

2.1. Fabrication of nanoCA

The nanoCA was fabricated by nanoimprint with diameter of ~200 nm and deposited with Au nanoparticles in diameter of ~10 nm (Gartia et al., 2013). The nanocone template made on plastic substrate was passivated with dimethyl dichlorosilane solution for 30 min, and rinsed by ethanol and deionized water. A 250 μm thick flexible (poly)ethylene terephthalate (PET) sheet was used as supporting substrate, and a Teflon roller was used for evenly distributing the UV curable polymer on the template. A UV light-curing flood lamp system (EC-Series, Dymax, USA) with average power density of 105 mW cm^{-2} was used to cure the UV polymer for 60 s at room temperature. A six pocket e-beam evaporation system (FC/BJD2000, Temescal, USA) was used for the Au evaporation. A thin adhesive layer of titanium (5 nm) was deposited before the evaporation of Au nanoparticle film (50 nm). Fig. 1a showed photograph of nanoCA device and nanostructure image of scanning electron microscope (SEM, XL30-ESEM, Philips, Netherland).

2.2. LSPR measurement

As shown in Fig. 1b, the optical detection system was constructed with a halogen cold light source (DT-MINI-2, Ocean Optics Inc., Dunedin, USA), a spectrophotometer (USB2000+, Ocean Optics Inc., Dunedin, USA) and two fiber bundles. The halogen cold light source and spectrophotometer were connected to the light emitting probe and the receptor probe respectively with fibers. The nanoCA was immobilized on the bottom of transparent electrochemical reactor. The emitting probe and receptor probe were respectively fixed below and above the reactor with metal

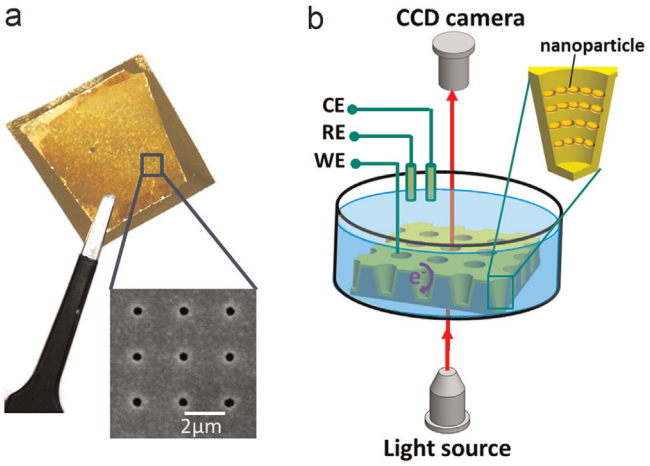

Fig. 1. The nanoCA for electrochemical and LSPR measurement. (a) Photograph of nanoCA device in ~2 × 2 cm^2 with the SEM image. The diameter of nanoCA was approximately 500 nm. Au nanoparticles on the surface of nanoCA were in diameter of ~50 nm. (b) Schematic of experimental apparatus for synchronous electrochemical and optical measurement. A standard three-electrode system was fabricated with nanoCA device (working electrode, WE), Ag/AgCl electrode (reference electrode, RE) and platinum electrode (counter-electrode, CE) for electrochemical reaction. Optical detection was performed in parallel with transmission spectrum. The light source was below nanoCA device. The light was delivered through nanoCA and finally received with a CCD.

frame, both keeping 1 cm away from the reactor. With the calibration of collimating lens, the light from the emitting probe to the receptor probe was kept in vertical straight. In the measurement, after emitted from the source and delivered through the nanoCA device, the light was finally received by a CCD. The LSPR signal was measured and analyzed in transmission spectrum. The range of transmission spectrum was from 300 nm to 1000 nm with step of 0.5 nm. The transmission spectrum was recorded when the surface of nanoCA had RI change and electrochemical current. The shift in LSPR peak and dip could be extracted from the transmission spectrum and used to transduce signals.

2.3. Electrochemical measurement

The electrochemical reactions were measured by electrochemical workstation (CHI660E, Chenhua, China) in a standard three-electrode system. In our experiments, the potentiodynamic electrochemical measurement of cyclic voltammetry (CV) was used to investigate the electrochemistry properties of nanoCA device and the electrochemical modulation to LSPR. The nanoCA device was used as working electrode, while platinum electrode and Ag/AgCl electrode were used as counter-electrode and reference electrode respectively. The scanning rates of CV were all kept at 0.02 V/s. 5 mM $K_4[Fe(CN)_6]/K_3[Fe(CN)_6]$ (1:1) was employed as redox couple in aqueous solution for electrochemical characterization.

2.4. Electrochemical LSPR measurement for bio-detection

The apparatus for electrochemical LSPR measurement was depicted in Fig. 1b. The synchronous measurement of CV scanning and transmission spectrum were performed to study interactions between electrochemical current and LSPR. The scanning rate of CV was fixed on 0.02 V/s and transmission spectrum was recorded and saved every 5 s simultaneously. The transmission spectrum was obtained to represent optical LSPR, in the step of 0.1 V during voltage scanning with different electrochemical current. The instruments and other operations about synchronous

Please cite this article as: Zhang, D., et al., Biosensors and Bioelectronics (2014), http://dx.doi.org/10.1016/j.bios.2014.08.022

electrochemical and LSPR measurement were same as separate electrochemical and optical measurement.

In the detection utilizing direct electrochemical redox of biomolecule, bovine serum albumin (BSA) was measured at different concentrations in synchronous electrochemical and LSPR measurement described above. It was dissolved in phosphate buffered saline (PBS, pH=7.4) at concentration of 1 mg/ml and saved under 4 °C. In the direct detections for BSA at different concentrations, BSA solution was diluted to 10 μg/ml, 25 μg/ml, 50 μg/ml, 75 μg/ml and 100 μg/ml with PBS.

Besides the direct electrochemical detection, a biosensor was designed for specific binding of BSA to its antibody (anti-BSA). Before detection, 10 μg/ml anti-BSA was incubated on the nanoCA for 60 min under 4 °C. Then, BSA at 100 μg/ml was detected by the biofunctionalized nanoCA, with human serum albumin (HSA) detected as negative protein. In the measurement, 5 mM $K_4[Fe(CN)6]/K_3[Fe(CN)6]$ (1:1) was used as redox couple to generate redox current for electrochemical and optical measurements.

Reagents in the experiments were all purchased from Sigma-Aldrich (USA).

3. Results

3.1. LSPR measurement for nanoCA

The nanoCA device was subwavelength opening on plastic substrate and decorated with Au nanoparticles in diameter of ~10 nm by electron beam evaporation. The hybrid device of nanoparticles and nanocups offered LSPR mediated by surface plasmon polariton-Bloch wave (SPP-BW), Wood's anomaly (WA) and Mie scattering (Gartia et al., 2013). In measurement, transmission spectrum from nanoCA was recorded and used to evaluate LSPR on the surface of nanoCA. The LSPR shift in wavelength could be observed in transmission spectrum when RI of medium was changed on the surface of nanoCA. In the experiment, analyte solutions were added on the surface of nanoCA, which changed RI and modulated optical transmission. Fig. 2a showed transmission spectrum of nanoCA to NaCl solutions at different concentrations with increasing RI. It was found that the whole transmission spectrum had red-shift (shift to right end of the spectrum) with NaCl, which indicated the RI sensitivity of nanoCA in LSPR detection. The statistic in Fig. 2b indicated that the wavelengths of LSPR peaks and dip in transmission spectrum all had the same shifts with whole transmission in presence of NaCl. These shifts in wavelength could be used to analyze RI changes. The resonance wavelength shifts with NaCl at increasing concentrations showed a high sensitivity of nanoCA for RI change with ~104 nm per RI unit.

3.2. Electrochemical LSPR for nanoCA

Electrochemistry is a powerful analytical method that has been used for a wide range of applications from chemical analysis to biological monitoring. Among various electrochemical measuring methods, cyclic voltammetry was generally used to study electrochemical properties of electrode and analyte, while gold electrodes were widely used in electrochemical bio-detections because of their good biological affinity (Bryan et al., 2013; Wang, 2008; Xia et al., 2013). In our electrochemical LSPR sensing, the nanoCA with Au nanoparticle film was used as working electrode to produce electrochemical reaction with Ag/AgCl reference electrode and Pt counter-electrode. Although the CV curves of nanoCA had lower electrochemical current than that of bare gold electrode, the voltammogram of nanoCA and gold electrode shared the same characteristic redox peaks (Fig. 3). The lower current of nanoCA may attribute to the poorer electrical conductivity of plastic

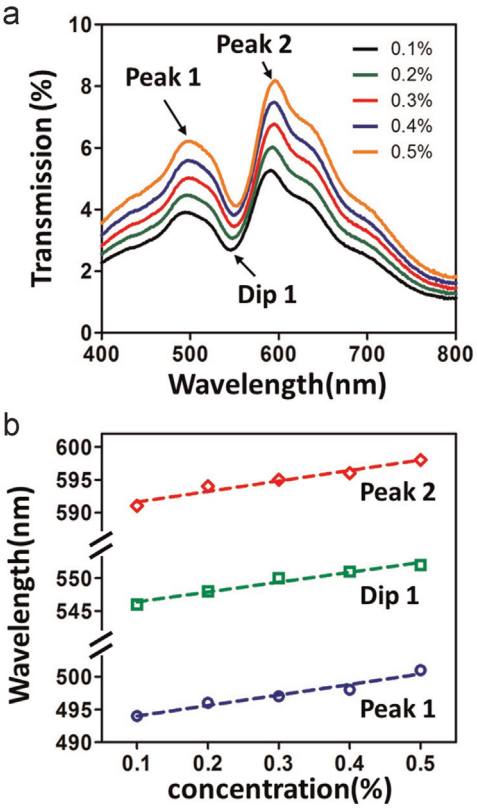

Fig. 2. LSPR measurement of nanoCA. (a) Transmission spectrum of nanoCA in presence of NaCl at concentration from 0.1% to 0.5% with increasing RI. The LSPR peak and dip were right shifted in increment of NaCl. (b) Wavelength shifts in peak and dip elicited by RI changes on nanoCA. The peaks and dip in transmission spectrum were marked with Peak 1, Dip 1 and Peak 2 respectively. The LSPR wavelengths at Peak 1 (blue), Dip1 (green) and Peak2 (red) increased with the concentrations of NaCl. (For interpretation of the references to color in this figure legend, the reader is referred to the web version of this article.)

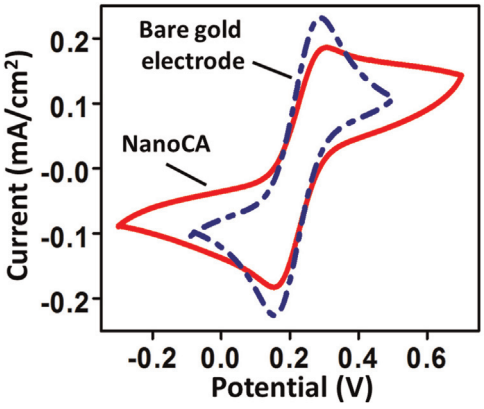

Fig. 3. Electrochemical property of nanoCA. NanoCA (red line) and conventional gold electrode (blue dashed) were compared as working electrodes in CV scanning. NanoCA device and gold electrode shared similar voltammogram and same characteristic redox peaks around 0.2 V. (For interpretation of the references to color in this figure legend, the reader is referred to the web version of this article.)

substrate in the fabrication of nanoCA. However, the same characteristic redox peaks of nanoCA and bare gold electrode demonstrated nanoCA shared similar electrochemical characteristics with conventional gold electrodes. Therefore, nanoCA could be used as working electrode in electrochemical reaction like other gold electrodes.

In the investigations about electrical properties of nanostructures, some groups reported that the potential and current can

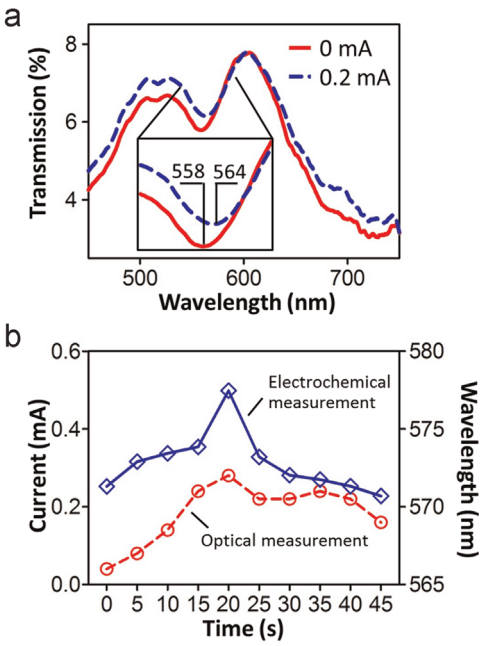

Fig. 4. Electrochemical LSPR measurement on nanoCA. (a) Interactions between electrochemical and LSPR measurement. The LSPR dip was right shifted in transmission spectrum when electrochemical current of 0.2 mA was applied. The significant shift was observed from 566 nm to 572 nm. (b) Synchronous measurement of LSPR and electrochemistry in CV scanning. The LSPR wavelength shift increased with electrochemical current from 0 s to 20 s, and decreased after 20 s. (For interpretation of the references to color in this figure legend, the reader is referred to the web version of this article.)

change LSPR output of nanostructures such as nanoparticles and nanodisks (Dahlin et al., 2011; Sannomiya et al., 2010). In our experiments, the electrochemical LSPR measurement was applied to LSPR of nanoCA in presence of electrochemical currents. The measurements were carried out with LSPR transmission spectrum and synchronous CV scanning. As seen in Fig. 4a, a significant LSPR dip shift could be observed in transmission spectrum when electrochemical current on nanoCA surface was changed from 0 mA to 0.2 mA. The resonance wavelength was shifted from 558 nm to 564 nm. But, there was no significant shift observed for LSPR peaks. The wavelength shifts of LSPR dips in optical measurement were shown in Fig. 4b within CV scanning. During the scanning, the wavelength of dip was shifted from 566 nm to 573 nm with the increase of current from 0.25 mA to 0.5 mA. When the current returned to 0.25 mA, the wavelength also decreased with current in decline phase. These results indicated that the current change on the nanoCA surface could modulate LSPR of nanoCA and offer wavelength shift in LSPR. The LSPR in transmission dip around 550 nm could be enhanced by electrochemical current and could be analyzed as an indicator in electrochemical LSPR detecting.

3.3. Bio-detection with electrochemical LSPR

Utilizing electrochemical enhancement for LSPR on nanoCA, electrochemical LSPR biosensor can be fabricated with a higher sensitivity in the synchronous measurement. Many biomolecules, such as proteins and nucleic acids, have special redox peaks in current during electrochemical scanning in biological and chemical sensing (Fan et al., 2003; Li et al., 2012; Shan et al., 2009). The redox current on surface of device would bring extra dip shift in wavelength in transmission spectrum and enhance optical LSPR signals from biomolecules. In this study, the detection of direct electrochemical redox of BSA was used as the applying demonstration of the enhancement of electrochemical LSPR sensor in bio-detections. In order to successfully record optical signals at point of redox peak in electrochemical reaction, CV was carried out with BSA at different concentrations in PBS. In Fig. 5a, the redox peaks of BSA were observed at 0.6 V in voltammogram. The currents of redox peaks increased with the concentrations of BSA. Based on electrochemical LSPR measurement, the increasing redox current brought increasing LSPR dip shift and enhanced LSPR signals elicited by BSA on nanoCA. Electrochemical enhanced LSPR signals were obtained in optical measurement. With 100 μg/ml BSA, the transmission spectrum of nanoCA with CV scanning was illustrated in Fig. 5b. The transmission spectrum was recorded at 30 s later than the beginning of CV scanning, when the redox peak was reached around 0.6 V in the cyclic voltammogram. Compared to PBS, the LSPR dip in the transmission spectrum with BSA only shifted with 6 nm in absence of CV scanning. The shift in wavelength was only caused by RI change on nanoCA surface from BSA in PBS. However, the LSPR dip shift was enlarged to 13 nm with combined effect of electrochemical current from redox peak in CV scanning. The statistics for LSPR dip shifts in electrochemical enhancement were shown in Fig. 5c. For electrochemical-enhanced LSPR biosensor, the electrochemical current at redox peak almost doubled LSPR dip shift for BSA at every concentration in comparison to single LSPR measurement. The detection limits of the measurements with and without electrochemical scanning were 13 μg/ml and 25 μg/ml respectively with 3δ/slope calculation, while the standard deviations were 0.408 nm and 0.524 nm in the measurement compared to PBS. The biosensor had a lower detection limit and higher sensitivity than those of single LSPR

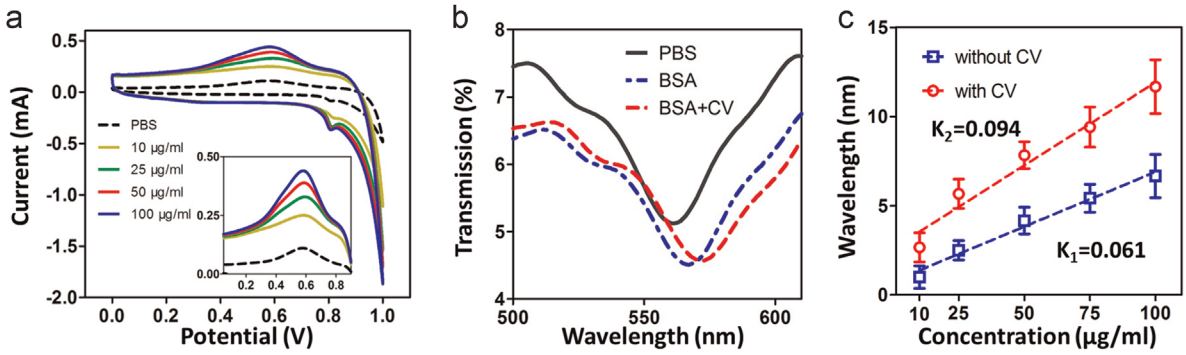

Fig. 5. Electrochemical LSPR detection utilizing direct electrochemical redox. (a) Electrochemical CV scanning for PBS and BSA at 10 μg/ml, 25 μg/ml, 50 μg/ml, 75 μg/ml and 100 μg/ml. (b) The transmission spectrum of nanoCA with PBS, 100 μg/ml BSA and BSA plus synchronous CV scanning. The wavelengths in LSPR dips were 561 nm, 567 nm and 574 nm respectively. (c) Statistic for shifts in dip wavelength from optical measurement with and without CV scanning. The optical signals of BSA at different concentrations with CV scanning (red circles) showed greater responses than those without CV scanning (blue squares). PBS was used as blank control (mean ± SD, $n=6$). (For interpretation of the references to color in this figure legend, the reader is referred to the web version of this article.)

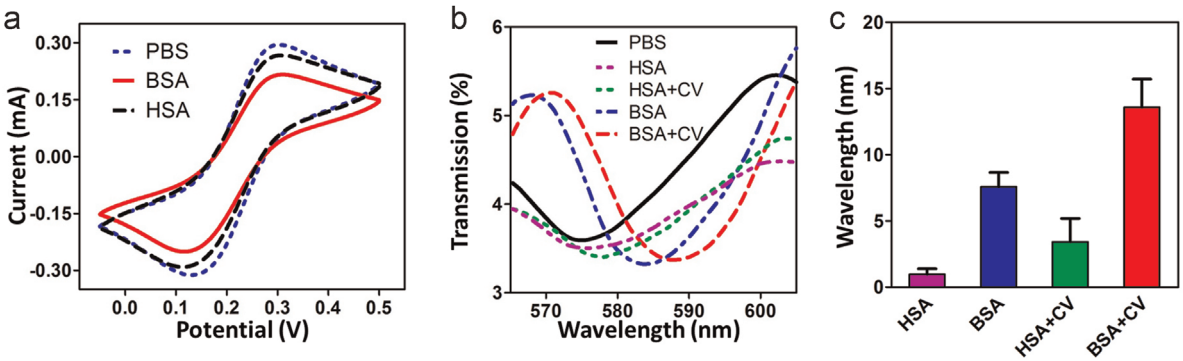

Fig. 6. Electrochemical LSPR detection utilizing specific binding of proteins. (a) Electrochemical CV scanning for PBS, BSA and HSA at 100 μg/ml. (b) The transmission spectrum of nanoCA with PBS, 100 μg/ml HSA and HSA plus CV scanning, 100 μg/ml BSA and BSA plus synchronous CV scanning. The wavelengths in LSPR dips were 575 nm, 576 nm, 578 nm, 584 nm and 590 nm respectively. (c) Statistic for shifts in dip wavelength of HSA, HSA plus CV, BSA and BSA plus CV. PBS was used as blank control (mean ± SD, $n=6$).

detection. These results suggested that the electrochemical coupled LSPR measurement had redox current to modulate LSPR dip shift besides that from RI change of solution and enhanced LSPR signals. The electrochemical-enhanced biosensor fabricated with electrochemical LSPR had greater responses and sensitivities than that of conventional optical methods.

Although electrochemical scanning could provide some level of selectivity, the biosensor would be interfered with substances owing similar electrochemical properties to the protein. The specific bindings between biomolecules were most common methods to obtain detecting selectivity. In our work, an antibody based biosensor was further designed for protein sensing. The nanoCA was modified by anti-BSA which could specifically bind to BSA. Different from the direct electrochemical detection, $K_4[Fe(CN)_6]/K_3[Fe(CN)_6]$ was added into the aqueous solution as redox couple. The redox current was generated from the redox couple and modulated by the binding of BSA to anti-BSA. As shown in Fig. 6a, the CV scanning provided redox current around 0.1 V and 0.3 V in the voltammogram with electrochemical reactions. The transmission spectrum was recorded when CV scanning reached 0.3 V (Fig. 6b). It showed that the LSPR dip shifts were elicited by the conjunction of anti-BSA and BSA on the surface of nanoCA and enhanced by the CV scanning from 9 nm to 15 nm. Due to the redox current, the negative protein of HSA also elicited wavelength shift about 3 nm in the measurement. However, it was much lower than the response to BSA about 15 nm with electrochemical enhancement (Fig. 6c). The results indicated that the biosensor kept both the electrochemical enhancement to LSPR signals and the selectivity to the protein. Thus, the electrochemical LSPR measurement could be applied in various selective detections utilizing specific binding of biomolecules.

4. Discussions

4.1. Interaction between LSPR and electrochemistry

In our study, optical LSPR measurement with electrochemical scanning was used to fabricate sensors to show multiply information from electrochemical and optical transducers simultaneously. It allowed us to investigate the interactions between electrochemistry and LSPR on nanostructures such as nanoCA. Investigations about electrochemical SPR have demonstrated that electrochemical reaction can change redox species around gold surface of SPR devices and then modulate optical responses in synchronous effects of electrochemistry and optics (Shan et al., 2010; Wang et al., 2010). Especially, quantitative relationships between electrochemical SPR signal and electrochemical current on surface have been established in the above investigations. Similar to electrochemical SPR, the electrochemical scanning in LSPR could also change redox reaction species around the nanoCA surface, elicit RI changes and finally generate extra LSPR wavelength shifts in transmission spectrum in this study. More interestingly, the electrochemical LSPR shift could only be observed in dip in transmission spectrum, while the peaks in transmission spectrum had no significant shifts in wavelengths. It may be due to that the peak and dip in transmission spectrum were elicited by different physical optical phenomenon. The dip was generated by SPP-BW, while two peaks were caused by WA and Mie scattering respectively (Gartia et al., 2013; Henzie et al., 2009). The SPP-BW was propagating SPP modes on periodically structured surface of nanoCA, which was much different from nonpropagating properties of WA and Mie scattering from the single nanostructure such as nanohole and nanoparticle. Due to periodical array structure on our device, the redox reaction had more influence on enhancement for LSPR dip in electrochemical LSPR sensing. Thus, the LSPR dip shift could be recorded with electrochemical enhancement and used to analyze in electrochemical LSPR detection with nanoCA.

However, mechanisms of the interaction between electrochemistry and LSPR were complex. In our experiment, the nonlinear change between optical and electrochemical responses was observed after 20 s in Fig. 4b. The RI difference and surface dielectric function could be influenced by several factors such as electron density, electrical attraction and temperature in the electrochemical scanning (Dahlin et al., 2012). For example, the electrochemical activity could potentially heat the metal and cause changes in the dielectric function, which might give rise to the extra wavelength shifts. Similarly, the continuous positive voltage would also change ion concentration around the nanoCA and then elicit wavelength shifts. Thus, optical and electrochemical responses might not keep paralleled change in the CV scanning. However, in the bio-detection, the optical signals were recorded at the redox current peak in the voltammogram, where significant redox reactions happened. The nonlinear relationship between optical and electrochemical responses in the decreasing phase had little influence on the performance of electrochemical LSPR sensor.

4.2. Electrochemical LSPR measurement in bio-detection

Although electrical effects on LSPR were reported by several groups, there were only a few synergetic sensing systems based on combination of electrochemistry and LSPR from nanostructures actually in use as sensors (Dahlin et al., 2012). In our study, utilizing the electrochemical-enhanced LSPR, the LSPR measurement coupled with electrochemistry could be applied in bio-detection for

biomolecule such as BSA. The nanoCA device had a high sensitivity about ~104 nm per RIU, which was much higher than 522 nm per RIU and 406.4 nm per RIU of the similar LSPR devices of nanoholes applied in bio-detections (Jia et al., 2013; Kee et al., 2013). It was used as electrochemical working electrode and optical LSPR transducer in parallel. In direct bio-detection, the electrochemical LSPR sensor showed greater response and sensitivity than that of single LSPR measurement. The LSPR signals were enhanced in extra dip shift by redox current. In fact, the generations of special redox currents were determined by electrocatalysis of material as working electrode. Although nanoCA had the poorer conductivity than conventional gold electrode, it had a better electrocatalysis for analytes with Au nanoparticles on nanoCA. Several groups had reported the excellent electrocatalysis abilities of nanoparticles for various chemicals and biomolecules (Magro et al., 2014; Sharifi et al., 2013; Welch and Compton, 2006). Thus, in addition to BSA, the electrochemical LSPR sensor also could be used in bio-detection for molecules such as DNA, enzyme and antibody with great electrocatalysis of Au nanoparticles in the electrochemical enhanced measurements. Besides the electrochemical selectivity, biological modification was another common method applied widely in biosensor design. In our study, the selective detection for BSA was further demonstrated by the sensor modified with its antibody, while keeping the electrochemical enhancements for LSPR signals. Thus, the electrochemical LSPR measurement could be used in various biosensors utilizing the specific binding between biomolecules, to achieve more selective detections.

Furthermore, the electrochemical scanning also had another excellent biosensing effects in LSPR measurement. The negatively charged proteins can attach to positively charged surfaces (Molina-Bolívar and Ortega-Vinuesa, 1999; Rabe et al., 2011). Thus, besides redox current, electrochemical scanning provided the positive potential to concentrate analytes on the surface. In above bio-detection, the BSA with negative charge could be attached on the surface of nanoCA with positive potential. The attachment would increase BSA concentrations around the sensor surface and then bring larger RI changes. Therefore, the electrochemical LSPR sensor also has potential applications in detection for chemicals without significant electrochemical reactions with electrode. At the same time, the electrochemical selectivity was another issue that can be investigated in the electrochemical LSPR sensor. The SPR and LSPR sensors often should be modified with chemical film or biomolecules to obtain the selectivity to analytes (Cao et al., 2014; Jeon et al., 2011; Mayer and Hafner, 2011). The modification process was often complex and the sensors usually had to be re-modified for each detection. However, combined with synchronous electrochemistry, the electrochemical LSPR sensor can detect some special chemicals with the electrochemical selectivity and may avoid the complex re-modification before measurements.

5. Conclusion

In summary, we developed an electrochemical LSPR sensor based on electrochemical coupled LSPR measurement on nanocups. The interaction between electrochemistry and LSPR on nanoCA was studied in the synchronous detection. The electrochemical enhancement for LSPR was observed on nanoCA and then utilized in bio-detection for BSA as applying demonstration. The electrochemical LSPR biosensor had a larger response and greater sensitivity than those of conventional LSPR measurement. The electrochemical LSPR on nanostructure will provide novel approaches to design biosensors with greater sensitivity and selectivity.

Acknowledgments

This work was supported by the National Natural Science Foundation of China (Grant no. 81371643), the Zhejiang Provincial Natural Science Foundation of China (Grant nos. LR13H180002, Y12H280002, and Q12H280001), and the Fundamental Research Funds for the Central Universities (Grant nos. 2014FZA5018 and 2014XZZX006-06).

References

Baba, A., Taranekar, P., Ponnapati, R.R., Knoll, W., Advincula, R.C., 2010. ACS Appl. Mater. Interfaces 2 (8), 2347–2354.
Bryan, T., Luo, X., Bueno, P.R., Davis, J.J., 2013. Biosens. Bioelectron. 39 (1), 94–98.
Cao, J., Sun, T., Grattan, K.T.V., 2014. Sens. Actuators B: Chem. 195, 332–351.
Cheng, X.R., Hau, B.Y.H., Endo, T., Kerman, K., 2014. Biosens. Bioelectron. 53, 513–518.
Dahlin, A.B., Dielacher, B., Rajendran, P., Sugihara, K., Sannomiya, T., Zenobi-Wong, M., Vörös, J., 2012. Anal. Bioanal. Chem. 402 (5), 1773–1784.
Dahlin, A.B., Sannomiya, T., Zahn, R., Sotiriou, G.A., Vörös, J., 2011. Nano Lett. 11 (3), 1337–11343.
Fan, C., Plaxco, K.W., Heeger, A.J., 2003. Proc. Natl. Acad. Sci. USA 100 (16), 9134–9137.
Gartia, M.R., Hsiao, A., Pokhriyal, A., Seo, S., Kulsharova, G., Cunningham, B.T., Bond, T.C., Liu, G.L., 2013. Adv. Opt. Mater. 1 (1), 68–76.
Henzie, J., Lee, J., Lee, M.H., Hasan, W., Odom, T.W., 2009. Annu. Rev. Phys. Chem. 60, 147–165.
Homola, J., 2008. Chem. Rev. 108 (2), 462–493.
Jeon, B.-J., Kim, M.-H., Pyun, J.-C., 2011. Sens. Actuators B: Chem. 154 (2), 89–95.
Jia, P., Jiang, H., Sabarinathan, J., Yang, J., 2013. Nanotechnology 24 (19), 195501.
Kee, J.S., Lim, S.Y., Perera, A.P., Zhang, Y., Park, M.K., 2013. Sens. Actuators B: Chem. 182, 576–583.
Li, Y., Zhong, Z., Chai, Y., Song, Z., Zhuo, Y., Su, H., Liu, S., Wang, D., Yuan, R., 2012. Chem. Commun. 48 (4), 537–539.
Liron, Z., Tender, L.M., Golden, J.P., Ligler, F.S., 2002. Biosens. Bioelectron. 17 (6–7), 489–494.
Magro, M., Baratella, D., Salviulo, G., Polakova, K., Zoppellaro, G., Tucek, J., Kaslik, J., Zboril, R., Vianello, F., 2014. Biosens. Bioelectron. 52, 159–165.
Mayer, K.M., Hafner, J.H., 2011. Chem. Rev. 111 (6), 3828–3857.
Molina-Bolívar, J.A., Ortega-Vinuesa, J.L., 1999. Langmuir 15 (8), 2644–2653.
Pallarola, D., Schneckenburger, M., Spatz, J.P., Pacholski, C., 2013. Chem. Commun. 49 (75), 8326–8328.
Rabe, M., Verdes, D., Seeger, S., 2011. Adv. Colloid Interface Sci. 162 (1–2), 87–106.
Sannomiya, T., Dermutz, H., Hafner, C., Vörös, J., Dahlin, A.B., 2010. Langmuir 26 (10), 7619–77626.
Shan, C., Yang, H., Song, J., Han, D., Ivaska, A., Niu, L., 2009. Anal. Chem. 81 (6), 2378–2382.
Shan, X., Díez-Pérez, I., Wang, L., Wiktor, P., Gu, Y., Zhang, L., Wang, W., Lu, J., Wang, S., Gong, Q., 2012. Nat. Nanotechnol. 7 (10), 668–672.
Shan, X., Patel, U., Wang, S., Iglesias, R., Tao, N., 2010. Science 327 (5971), 1363–1366.
Sharifi, E., Salimi, A., Shams, E., 2013. Biosens. Bioelectron. 45, 260–266.
Stewart, M.E., Anderton, C.R., Thompson, L.B., Maria, J., Gray, S.K., Rogers, J.A., Nuzzo, R.G., 2008. Chem. Rev. 108 (2), 494–521.
Tokel, O., Inci, F., Demirci, U., 2014. Chem. Rev. 114, 5728–5752.
Wang, J., 2008. Chem. Rev. 108 (2), 814–825.
Wang, S., Huang, X., Shan, X., Foley, K.J., Tao, N., 2010. Anal. Chem. 82 (3), 935–941.
Welch, C.M., Compton, R.G., 2006. Anal. Bioanal. Chem. 384 (3), 601–619.
Xia, N., Deng, D., Zhang, L., Yuan, B., Jing, M., Du, J., Liu, L., 2013. Biosens. Bioelectron. 43, 155–159.
Yu, H., Shan, X., Wang, S., Chen, H., Tao, N., 2014. ACS Nano 8 (4), 3427–3433.
Zeng, S., Yong, K.-T., Roy, I., Dinh, X.-Q., Yu, X., Luan, F., 2011. Plasmonics 6 (3), 491–506.
Zhang, N., Schweiss, R., Zong, Y., Knoll, W., 2007. Electrochim. Acta 52 (8), 2869–2875.